Electrical signature in polar night cloud base variations

2013 Environ. Res. Lett. 8 015027

(http://iopscience.iop.org/1748-9326/8/1/015027)

OPEN ACCESS
IOP PUBLISHING
ENVIRONMENTAL RESEARCH LETTERS
Environ. Res. Lett. **8** (2013) 015027 (7pp)
doi:10.1088/1748-9326/8/1/015027

Electrical signature in polar night cloud base variations

R Giles Harrison and Maarten H P Ambaum

Department of Meteorology, University of Reading, PO Box 243, Earley Gate, Reading, Berks RG6 6BB, UK

E-mail: r.g.harrison@reading.ac.uk

Received 17 September 2012
Accepted for publication 11 February 2013
Published 5 March 2013
Online at stacks.iop.org/ERL/8/015027

Abstract
Layer clouds are globally extensive. Their lower edges are charged negatively by the fair weather atmospheric electricity current flowing vertically through them. Using polar winter surface meteorological data from Sodankylä (Finland) and Halley (Antarctica), we find that when meteorological diurnal variations are weak, an appreciable diurnal cycle, on average, persists in the cloud base heights, detected using a laser ceilometer. The diurnal cloud base heights from both sites correlate more closely with the Carnegie curve of global atmospheric electricity than with local meteorological measurements. The cloud base sensitivities are indistinguishable between the northern and southern hemispheres, averaging a (4.0 ± 0.5) m rise for a 1% change in the fair weather electric current density. This suggests that the global fair weather current, which is affected by space weather, cosmic rays and the El Niño Southern Oscillation, is linked with layer cloud properties.

Keywords: atmospheric electricity, cosmic rays, cloud physics, space weather

1. Introduction

Low level layer (stratus) clouds provide, on average, about 29% of global cloud observed from the surface [1]. The formation of such layer clouds is primarily due to the local meteorological conditions, in which rising moist air cools until it becomes sufficiently supersaturated with water vapour to allow condensation on submicron diameter atmospheric particles. Growth of droplets from these small initial sizes occurs by water vapour diffusion, and collisions with other droplets. Droplet electrification also occurs at a layer cloud's lower edge [2], due to the 'fair weather' vertical atmospheric electric current flowing between the upper atmosphere and the surface [3]. Because of the abundance of layer clouds, the global presence of the vertical current could yield a small but widespread electrical influence perturbing layer cloud properties.

Changes have previously been inferred in the cloud base on timescales of minutes which have been associated with atmospheric electricity effects on cloud droplet behaviour [4–6], but direct experimental determination of an electrical response of cloud base droplets in layer clouds has not previously been reported. The cloud base zone is not amenable to satellite sounding, but information can be obtained experimentally using a standard laser cloud base recorder (ceilometer), which transmits near-infrared pulses of laser diode radiation upwards, and records the strength of the reflected signal against time. For the Vaisala CT25K ceilometer, the cloud base detection threshold is equivalent to a vertical visual range in cloud of 100 m, a definition of practical use to aircraft. Assuming typical cloud droplet concentrations of 50–200 cm^{-3}, visibility considerations [7] indicate this visual range criterion corresponds to cloud droplets of radii 5–10 μm. Hence, as at their initial formation droplets are of submicron size, the CT25K ceilometer responds to droplets which have grown in the weak updraught of the cloud. If the droplet formation height and updraught speed is, on average, steady, for example during prolonged polar night conditions when there is no

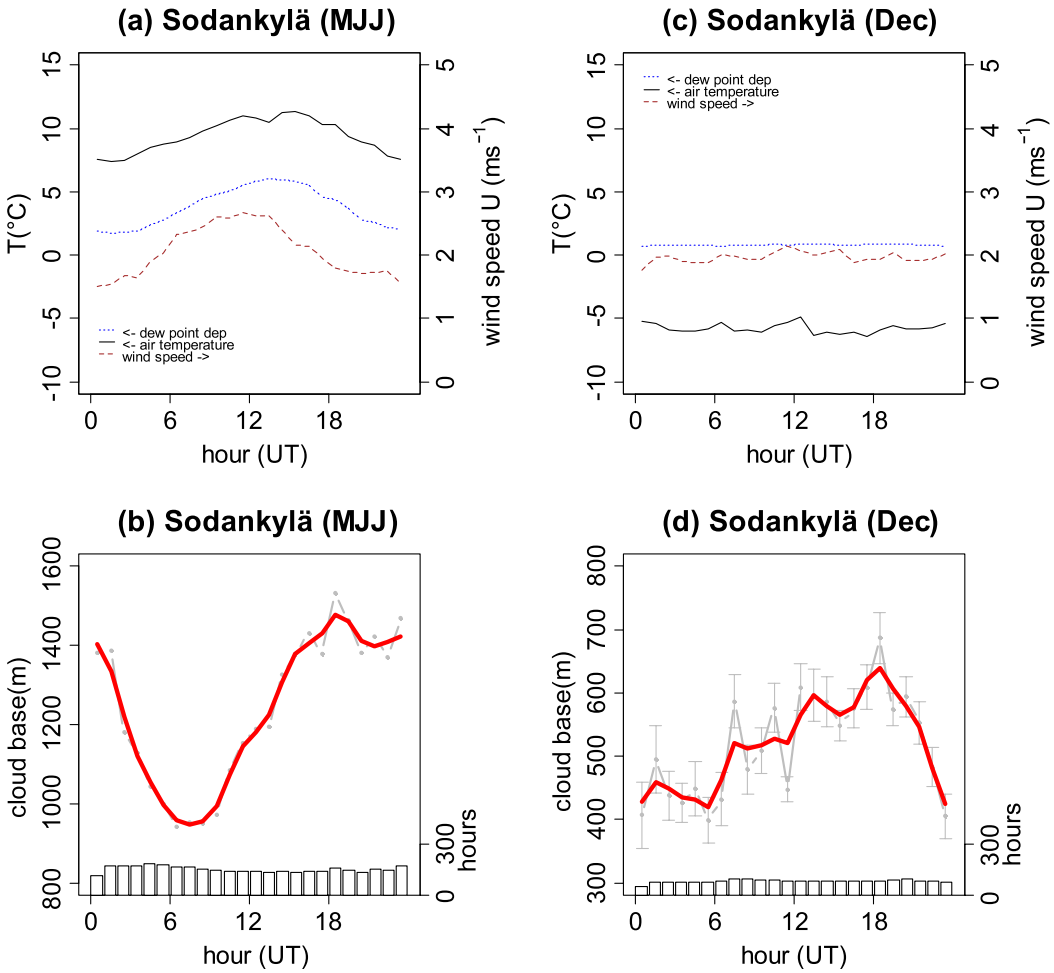

Figure 1. Mean hourly variations in air temperature, dew point temperature depression (T axis) and wind speed (U axis) for Sodankylä 2006–2011, in (a) local summer (May–June–July) and (c) polar twilight (December), calculated from automatic observations made every 1 min. (b) and (d) show the associated mean hourly height of the lowest detected cloud layer for the same circumstances as (a) and (c), calculated from all hourly cloud base height measurements below 4 km (red points). A smoothing line (weightings 1-2-1) has been added (thick red line), and error bars show one standard error, calculated after removing the derived diurnal cycle. The number of hours data in the averages is shown by the bar plot (right-hand axis).

diurnal cycle, the averaged ceilometer-detected cloud base provides a measurement of droplet growth variations. As a diurnal cycle in the vertical current is, on average, always present globally—the well-known 'Carnegie curve' of atmospheric electricity [8] shows a ±20% single cycle variation with a minimum around 3UT and maximum around 19UT [9–11]—polar winter ceilometer diurnal data offer a unique opportunity to evaluate any fair weather atmospheric electricity influence when other atmospheric variations are small.

2. Polar cloud base data

Ceilometer data from two high latitude sites in each hemisphere, from Sodankylä (Finland, 67.4 °N, 26.6 °E), and Halley (Antarctica, 75.5 °S 26.4 °W), are analysed for diurnal cycle information. Sodankylä is surrounded by wooded terrain, at 179 m above mean sea level; Halley is on the Brunt Ice Shelf, in the Weddell Sea. At Sodankylä, during December, the maximum day length is only 3 h, with only 31 min between sunrise and sunset on 19th/20th. Figure 1 compares mean surface meteorological conditions at Sodankylä during the local summer and December, and the cloud base height (H_{cb}) of the lowest cloud level detected with a CT25K ceilometer, with cloud above 4 km removed to exclude effects dominated by ice cloud. (This height is chosen as, below −40 °C, all supercooled liquid clouds become ice, and the temperature typically falls with height at less than ∼10 °C km^{-1}.) In the summer (figures 1(a) and (b)), a diurnal cycle is apparent in air temperature T_{air}, dew point depression ($T_{air} - T_{dew}$) (a quantity inversely proportional to humidity and to which cloud base height is related) and surface wind speed measured at 10 m, U_{10}, with a substantial associated diurnal variation in H_{cb}. Without appreciable daylight in December, (figures 1(c) and (d)), there is a much reduced T_{air} variation (1.5 °C diurnal maximum to minimum), and a variation in ($T_{air} - T_{dew}$) of 0.17 °C.

A similar comparison, but for the southern hemisphere using data from Halley is shown in figure 2, with ceilometer returns above 2 km removed to again restrict the comparison

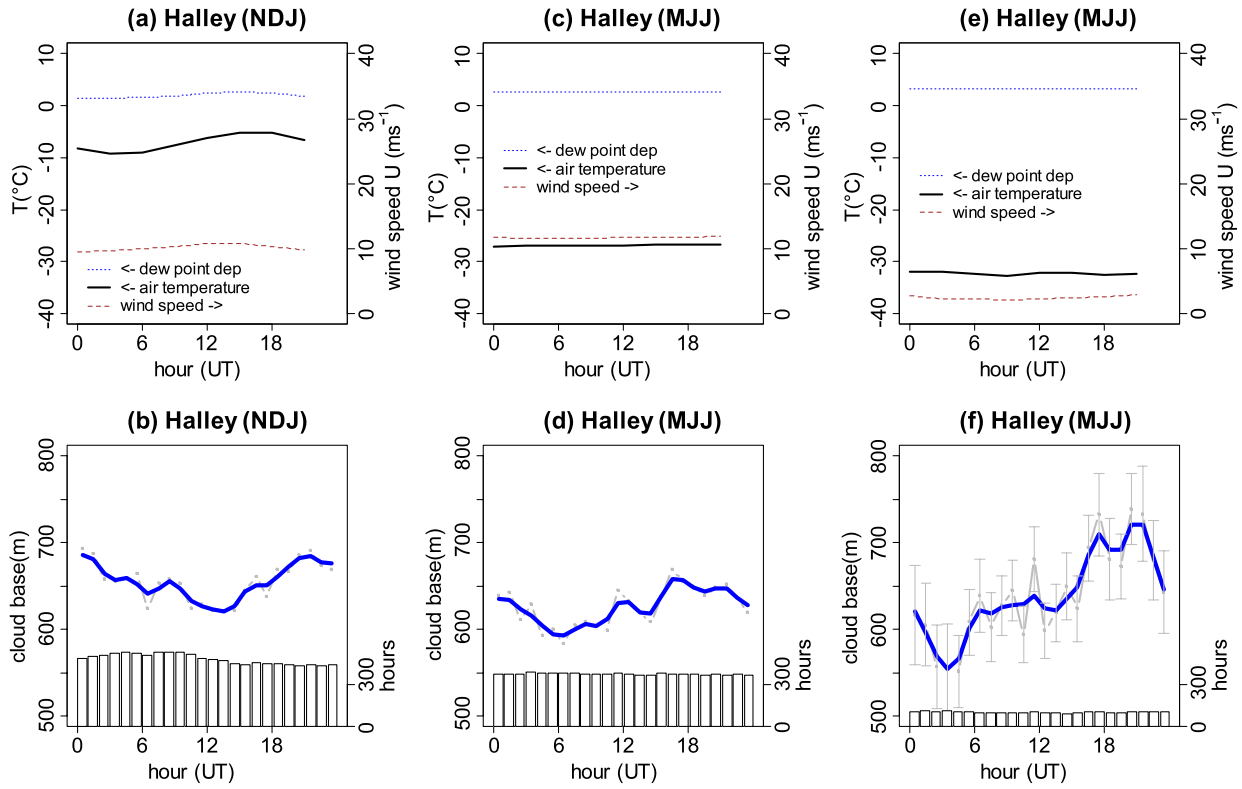

Figure 2. Mean diurnal cycles in surface meteorological quantities (air temperature, dew point depression and wind speed), at Halley, for (a) summer (November–December–January) and (c) winter (May–June–July), measured at 3-hourly intervals from 2003 to 2011. (e) also shows winter data, sub-selected from days with daily mean wind speeds in the lowest decile. (b), (d) and (f) give the associated mean hourly height of the lowest cloud level (blue lines), from cloud base below 2 km, calculated from 1 min (2003–2005) and 30 s samples (2005–2011). A smoothing line (weightings 1-2-1) has been added (thick black line), and error bars show one standard error, calculated after removing the derived diurnal cycle. The number of hours data in the averages is shown by the bar plot (right-hand axis).

to liquid cloud. During November, December and January, the sun is continuously above the horizon, and a mean diurnal cycle is apparent in U_{10}, T_{air} and $(T_{\mathrm{air}} - T_{\mathrm{dew}})$, the latter two quantities spanning, respectively 4.0 and 1.2 °C from maximum to minimum, figure 2(a). A diurnal cycle is also clearly present in H_{cb} (figure 2(b)), lagged on T_{air}. During the polar night between May and July the diurnal cycle in U_{10}, T_{air}, and $(T_{\mathrm{air}} - T_{\mathrm{dew}})$ disappears, the latter quantities only spanning 0.4 °C and 0.07 °C from maximum to minimum respectively. Nevertheless a cyclic variation in H_{cb} is still apparent, with a similar phase relationship to that of figure 1(a). Because wind speeds at Halley are much greater than at Sodankylä, a sub-selection of days at Halley during May–June–July having daily mean U_{10} in the lowest decile has also been considered to make the site conditions more comparable and diminish external meteorological influences (figures 2(e) and (f)). Despite the reduction in data from using just the lowest decile, the diurnal cycle in H_{cb} persists, with increased amplitude. Only the low wind speed cases will be considered further, to ensure that the cloud base effects are local. (Note that the semi-diurnal 'tidal' variations in pressure are small at these latitudes; for the conditions selected, the standard deviations of the mean hourly pressure are 0.2 hPa at Halley and 0.8 hPa at Sodankylä.)

3. Explanations for the diurnal cloud base variation

We now consider conventional meteorological explanations for the diurnal variations observed, followed by further consideration of the Carnegie curve. As evident from figure 2, the polar night variations in the meteorological quantities are small, so figure 3 provides them in greater detail. For the possible effects we investigate, firstly, their amplitudes, and, secondly, their phase relationships.

3.1. Amplitude

Figure 3 compares the averaged diurnal variations in cloud base at Halley and Sodankylä with the averaged diurnal variation in surface air temperature ((a) and (d)) and dew point depression ((b) and (e)). These surface quantities can be related to the cloud base height, as the cloud base corresponds to the altitude where the air becomes saturated, that is, where the dew point temperature T_{d} equals the air temperature T_{a}. The dew point depression, $T_{\mathrm{a}} - T_{\mathrm{d}}$, varies approximately with height as

$$\frac{\mathrm{d}(T_{\mathrm{a}} - T_{\mathrm{d}})}{\mathrm{d}z} = -\left(\Gamma - \frac{gR_{\mathrm{v}}T_{\mathrm{a}}}{R_{\mathrm{d}}L}\right) = -\tilde{\Gamma} \qquad (1)$$

where $\Gamma = -\mathrm{d}T_{\mathrm{a}}/\mathrm{d}z$ is the environmental lapse rate, g is the acceleration due to gravity, R_{v} and R_{d} the specific gas

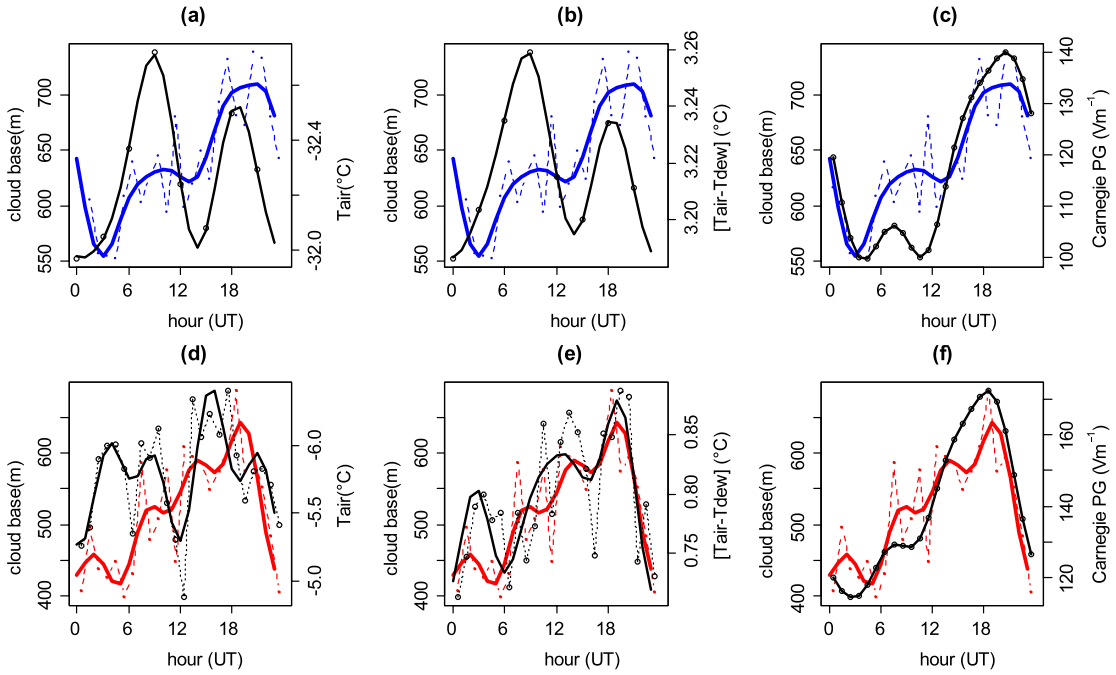

Figure 3. Hourly averaged ceilometer cloud base height in winter for Halley (during May–June–July, 2003–2011, for the lowest decile of wind speeds, blue lines), and Sodankylä (during December, 2006–2012, all wind speeds, red lines), compared with (a) and (d) local surface air temperature T_{air}, (b) and (e) local surface dew point depression ($T_{\mathrm{air}} - T_{\mathrm{dew}}$) and (c) and (f), the standard Carnegie curve Potential Gradient (PG) variation for May–June–July (c) and November–December–January (f). (The thick lines are harmonic fits in each case, fourth order harmonic fits when 24-hourly data points are available, but for the three-hourly Halley meteorological data, third order.)

Table 1. Range of fractional changes (from the inter-quartile range in each case) in cloud base height H_{cb}, dew point depression $T_{\mathrm{a}} - T_{\mathrm{d}}$ and lapse rate $\tilde{\Gamma}$, i.e. the terms in equation (3). (We use a conservative estimate for the mean value of $\tilde{\Gamma}$ of 5 °C km^{-1}.)

Fractional change in:	Cloud base height $\frac{\delta H_{\mathrm{cb}}}{H_{\mathrm{cb}}}$	Dew point depression $\frac{\delta(T_{\mathrm{a}}-T_{\mathrm{d}})}{T_{\mathrm{a}}-T_{\mathrm{d}}}$	Lapse rate $\frac{\delta T_{\mathrm{a}}}{H_{\mathrm{cb}}\tilde{\Gamma}}$
Sodankylä	0.27	0.13	0.19
Halley	0.12	0.01	0.10

constants for water vapour and dry air respectively and L the latent heat of evaporation for air [12]. Assuming that the right-hand side of equation (1) is approximately constant with altitude, we can estimate the cloud base height H_{cb} from the dew point depression at the surface and its lapse rate $\tilde{\Gamma}$ as

$$H_{\mathrm{cb}} = (T_{\mathrm{a}} - T_{\mathrm{d}})/\tilde{\Gamma}. \tag{2}$$

Equation (2) indicates that the fractional change in cloud base height H_{cb} depends on fractional changes in both the dew point depression and the dew point depression's lapse rate $\tilde{\Gamma}$. Explicitly, the fractional change in H_{cb} depends on a dew point depression term and lapse rate term,

$$\begin{aligned}\frac{\delta H_{\mathrm{cb}}}{H_{\mathrm{cb}}} &= \frac{\delta\,(T_{\mathrm{a}} - T_{\mathrm{d}})}{T_{\mathrm{a}} - T_{\mathrm{d}}} - \frac{\delta\tilde{\Gamma}}{\tilde{\Gamma}} \\ &\approx \frac{\delta(T_{\mathrm{a}} - T_{\mathrm{d}})}{T_{\mathrm{a}} - T_{\mathrm{d}}} - \frac{\delta T_{\mathrm{a}}}{H_{\mathrm{cb}}\tilde{\Gamma}}\end{aligned} \tag{3}$$

where $\tilde{\Gamma}$ is allowed to vary with the surface temperature T_{a}, which is the only meteorological parameter available to quantify variations in lapse rate.

We use this model to estimate the magnitude of the fractional variations in cloud base that could be attributed to meteorological variations, i.e. from variations in the dew point depression ($T_{\mathrm{a}} - T_{\mathrm{d}}$) and dew point depression lapse rate $\tilde{\Gamma}$. Table 1 summarizes the results. We find that the fractional change in the dew point depression is generally too small to explain the variations in the cloud base, while, the estimated fractional changes in lapse rate appears to be of the right order of magnitude if a conservative (i.e. small) choice is made for $\tilde{\Gamma}$.

3.2. Phase

We now consider the temporal variations of the surface meteorological parameters, the cloud base height, and the possible explanation provided by the Carnegie curve for the daily mean cloud base variations having a minimum around 3UT and maximum around 19UT. The Carnegie curve is conventionally represented by a Fourier expansion containing 24 h, 12 h, 8 h and 6 h terms, for which phases and amplitudes are available by season [13]. Figures 3(c) and (f) show Carnegie curves calculated for the relevant season using the Fourier coefficients for May–June–July and November–December–January. The four term harmonic curve fitted to the ceilometer data obtained from Halley (figure 3(c)), and Sodankylä (figure 3(f)) has been derived from a harmonic fit in the same way as for the Carnegie data.

Table 2. Temporal correlation with cloud base height of three predictors (dew point depression $T_a - T_d$, lapse rate $\tilde{\Gamma}$, and the Carnegie curve). Note that the Halley meteorological data is three-hourly, but that the Halley cloud base is hourly, so we provide correlations between the Carnegie curve and cloud base using the same times as the meteorological data, and also for all the hourly values.

Correlation with H_{cb}	Dew point depression	Lapse rate	Carnegie curve
Sodankylä (hourly data)	0.69	−0.30	0.80
Halley (three-hourly data)	0.30	−0.47	0.75 (three-hourly data) 0.78 (hourly data)

The temporal correlations of the three possible predictors (dew point depression, lapse rate, and Carnegie curve) can now be compared with the variations in cloud base height. The results are summarized in table 2. (Note that the meteorological fields at Halley are determined at three hour intervals, so there are only eight data points in this comparison.) We find that the temporal correlation with the Carnegie curve for both sites is excellent with an explained variance of around 60%. Only the dew point depression at Sodankylä comes reasonably close in terms of explained variance but, as shown above, its magnitude falls short by at least a factor of two despite a conservative choice of lapse rate.

From these analyses it appears that the Carnegie curve presents the best explanation at both sites for the observed diurnal variation in cloud base height.

4. Further discussion of the Carnegie curve

Originally, the Carnegie curve was identified in surface ocean air measurements of the atmospheric electric field (observed as the vertical potential gradient) [9], which results from the vertical fair weather current of the global circuit flowing through the finite conductivity of atmospheric air. The global circuit is sustained by currents flowing globally in the ionosphere and surface, generated by thunderstorms and shower clouds which vary diurnally, and, when their contributions are integrated, yield the Carnegie curve [9, 11, 14]. In regions without the strong charge separation of disturbed weather, conventionally regarded as 'fair weather' regions for atmospheric electricity, the global circuit is closed by a small current which flows vertically through the atmosphere [15], and through layer clouds [16]. The Carnegie curve has been widely observed, including at latitudes encompassing Halley and Sodankylä, such as in the fair weather current at the Amundsen–Scott South Pole station [17] (90.0 °S), as well as in the potential gradient at Vostok [18] (78.5 °S), Shetland [19] (60.2 °N), and Tromsø [20] (69.7 °N).

Small changes in the timing of the maximum around 19–20UT in both hemispheres' polar winter H_{cb} observations are also suggestive of the seasonal variations in the Carnegie curve. The time of the maximum from the ceilometer harmonic fit occurs at 2040UT for Halley (May–June–July) and 1910UT for Sodankylä (December). Although there is year to year variability, a similar change in the time of the Carnegie curve maximum across the year occurs found at Vostok [18], with a maximum at 2050UT for July–August and at 1830UT for November–December.

The amplitude agreement between the seasonal Carnegie curve and the ceilometer data is demonstrated quantitatively in figure 4, which shows the relationship between the ceilometer data, the surface meteorological data and the relevant seasonal Carnegie curve, from figure 3, combined for both sites. The mean cloud base heights, air temperatures and dew point depressions, which are site dependent, and the mean potential gradient, which also varies seasonally, are first removed. Note that figure 4(b) plots the data in the form expected from equation (2), i.e. testing a linear relationship between dew point depression and cloud base height. This should be compared with the alternative relationship of figure 4(c). As shown in table 2, the correlations between dew point depression and cloud base height for each site independently are poorer than between potential gradient and cloud base height. Furthermore, the relationship with the potential gradient is statistically indistinguishable between the sites (figure 4(c)). The gradients of the fitted lines are (3.3 ± 0.5) m $(\mathrm{V\ m^{-1}})^{-1}$ for Sodankylä, (2.8 ± 0.5) m $(\mathrm{V\ m^{-1}})^{-1}$ for Halley, with one standard error on the gradient quoted in each case, after first removing the diurnal cycle.

A physical explanation for the close agreement in phase and sensitivity between H_{cb} and the Carnegie curve for the two sites in opposite hemispheres may be related to the effect of the global circuit current on cloud droplet properties and interactions. The ceilometer detection of the cloud base height responds to cloud droplet properties as the laser light return is proportional to the total droplet area i.e. for N the number concentration of drops of effective mean radius r, to Nr^2. Droplet charging around the base of stratus clouds is directly proportional to J_c [5], which can affect droplet formation, droplet–particle and droplet–droplet collision and coalescence [21]. With such a global circuit hypothesis, the consistent responses between the two sites, averaging (3.1 ± 0.4) m $(\mathrm{V\ m^{-1}})^{-1}$ can be understood as a ceilometer-derived cloud base height variation with the fair weather conduction current density J_c flowing through the cloud. Assuming the current density and potential gradient are related by Ohm's law, with no variation, on average, in conductivity, proportional changes in potential gradient and current density are equal. Finding the proportional PG change as the PG anomaly divided by the relevant seasonal mean, combining both seasons' data gives the equivalent sensitivity in cloud base height as (4.0 ± 0.5) m/% change in J_c.

5. Conclusions

The close agreement of the diurnal cycle in the ceilometer response and the Carnegie curve away from influence of

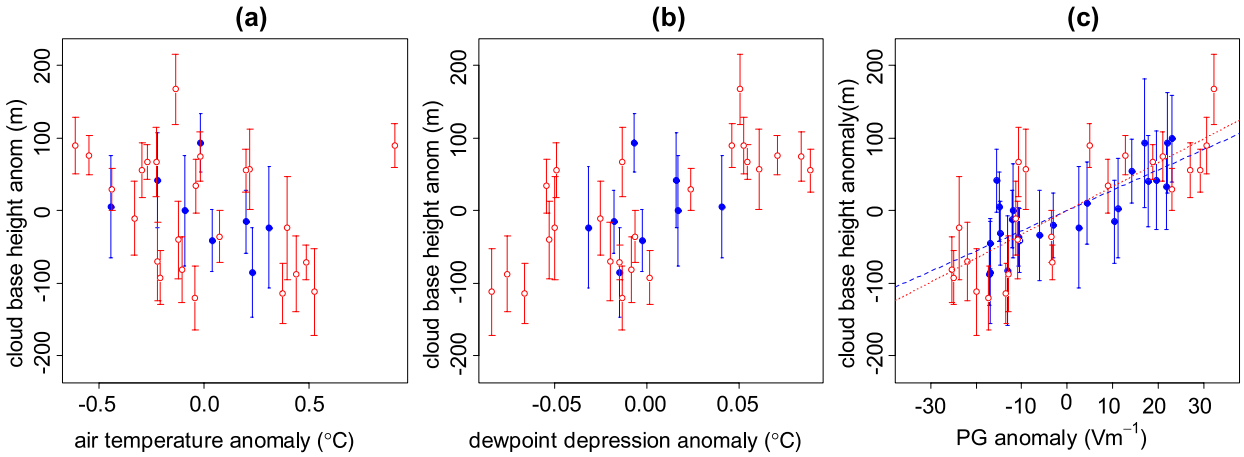

Figure 4. Hourly laser ceilometer cloud base height anomalies for both Halley (from figure 1(c), solid blue circles) and Sodankylä (from figure 1(f), hollow red circles), calculated by subtracting the mean cloud base (639.5 m for the Halley data and 519.4 m for the Sodankylä data) against, (a) air temperature anomaly (mean values: Sodankylä −5.8 °C and Halley −32.3 °C), (b) dew point depression anomaly (mean values: Sodankylä 0.8 °C and Halley 3.2 °C) and (c) potential gradient (PG) anomalies found similarly for the MJJ (mean PG 117 V m^{-1}) and NDJ (mean PG 140 V m^{-1}) seasons respectively. For (c), least squares fit lines have been added (Halley dashed, Sodankylä dotted). (Error bars are one standard error, calculated after removing the derived diurnal cycle in cloud base. Note that the Halley surface meteorological data is only provided at three-hourly intervals.)

solar radiation suggests direct coupling between the global circuit current and layer cloud properties becomes apparent when other sources of variability are weak. An estimate of its potential importance is that, for the ∼100 m change observed in the detected cloud base height related to the Carnegie curve, the associated cloud base temperature change would be about 1 K, or at least 1% in the down-welling long wave radiation at 250 K from Stefan's law, assuming no associated change in cloud base emissivity. Furthermore, if the cloud began precipitating, elevating the cloud base would allow more evaporation of falling small droplets, potentially suppressing drizzle reaching the surface. Both radiative and precipitation effects will average out across the diurnal cycle, but, because the global circuit current is also modulated by the external space environment [21] and cosmic rays [22], as well as internal climate variability such as the El Niño Southern Oscillation [19], identifying this electrical response in a cloud type of widespread extent hints at a role for the global circuit in climate teleconnections and solar-terrestrial effects on climate, and even potential applications in geo-engineering.

Finally, of the two mechanisms previously proposed to link cosmic rays with clouds [23], the first, through ion nucleation ('clear air'), which depends on selective atmospheric chemistry circumstances, seems increasingly to be considered as unimportant [24]. These findings present further evidence for the second ('near-cloud') group of mechanisms [3, 6, 21] between the global atmospheric electric circuit and the underlying physics of cloud droplets, in both hemispheres.

Acknowledgments

Meteorological data at Halley were obtained by the British Antarctic Survey (BAS), provided by the British Atmospheric Data Centre and S Colwell at BAS. The Finnish Meteorological Institute obtained and provided the Sodankylä meteorological measurements. Dr K A Nicoll (University of Reading) assisted with data.

References

[1] Klein S A and Hartmann D L 1993 The seasonal cycle of low stratiform clouds *J. Clim.* **6** 1587–606
[2] Nicoll K A and Harrison R G 2010 Experimental determination of layer cloud edge charging from cosmic ray ionisation *Geophys. Res. Lett.* **37** L13802
[3] Tinsley B A 2000 Influence of solar wind on the global electric circuit, and inferred effects on cloud microphysics, temperature and dynamics in the troposphere *Space Sci. Rev.* **94** 231–58
[4] Harrison R G and Ambaum M H P 2008 Enhancement of cloud formation by droplet charging *Proc. R. Soc. Lond.* A **464** 2561–73
[5] Harrison R G and Ambaum M H P 2009 Observed atmospheric electricity effect on clouds *Environ. Res. Lett.* **4** 014003
[6] Harrison R G, Ambaum M H P and Lockwood M 2011 Cloud base height and cosmic rays *Proc. R. Soc. Lond.* A **467** 2777–91
[7] Koschmieder H 1924 Theorie der horizontalen Sichtweite *Beitr. Phys. Frei. Atmos.* **12** 33–55
[8] Harrison R G 2013 The Carnegie curve *Surv. Geophys.* **34** 209–32
[9] Whipple F J W 1929 On the association of the diurnal variation of electric potential gradient in fine weather with the distribution of thunderstorms over the globe *Q. J. R. Meteorol. Soc.* **55** 1–17
[10] Rycroft M J, Israelsson S and Price C 2000 The global atmospheric electric circuit, solar activity and climate change *J. Atmos. Sol-Terr. Phys.* **62** 1563–76
[11] Liu C, Williams E R, Zipser E J and Burns G 2009 Diurnal variations of global thunderstorms and electrified shower clouds and their contribution to the global electrical circuit *J. Atmos. Sci.* **67** 309–23
[12] McIlveen R 1992 *Fundamentals of Weather and Climate* 2nd edn (London: Chapman and Hall)

[13] Torreson O W, Parkinson W C, Gish O H and Wait G R 1946 Oceanography-III. Ocean atmospheric–electric results *Scientific Results of Cruise VII of the Carnegie during 1928–1929 Under Command of Captain J.P. Ault* (*Carnegie Institution of Washington Publication* vol 568) (Washington, DC: Carnegie Institution of Washington) (http://archive.org/stream/oceanatmospheric00carn/oceanatmospheric00carn_djvu.txt)

[14] Rycroft M J, Harrison R G, Nicoll K A and Mareev E A 2008 An overview of Earth's global electric circuit and atmospheric conductivity *Space Sci. Rev.* **137** 83–105

[15] Wilson C T R 1906 On the measurement of the Earth–air current and on the origin of atmospheric electricity *Proc. Camb. Phil. Soc.* **13** 363–82

[16] Nicoll K A and Harrison R G 2009 Vertical current flow through extensive layer clouds *J. Atmos. Sol-Terr. Phys.* **71** 1219–21

[17] Cobb W E 1977 Atmospheric electric measurements at the South Pole *Electrical Processes in Atmospheres* ed H Dolezalek and R Reiter (Darmstadt: Steinkopf) pp 161–7

[18] Burns G B, Frank-Kamenetsky A V, Troshichev O A, Bering E A and Reddell B D 2005 Interannual consistency of bi-monthly differences in diurnal variations of the ground-level, vertical electric field *J. Geophys. Res.* **110** D10106

[19] Harrison R G, Joshi M and Pascoe K 2011 Inferring convective responses to El Niño with atmospheric electricity measurements at Shetland *Environ. Res. Lett.* **6** 044028

[20] Barlindhaug E 1935 Results of registrations of the atmospheric potential gradient at the auroral observatory Tromsø during the period March 1932–July 1933 *Geofysiske Publikasjoner* **10** 3–12 (www.ngfweb.no/docs/NGF_GP_Vol10_no12.pdf)

[21] Rycroft M J, Nicoll K A, Aplin K L and Harrison R G 2012 Recent advances in global electric circuit coupling between the space environment and the troposphere *J. Atmos. Sol-Terr. Phys.* **90–91** 198–211

[22] Markson R 1981 Modulation of the Earth's electric field by cosmic radiation *Nature* **291** 304–8

[23] Carslaw K S, Harrison R G and Kirkby J 2002 Cosmic rays, clouds and climate *Science* **298** 1732–7

[24] Carslaw K S 2009 Cosmic rays, clouds and climate *Nature* **460** 332